Biomaterials 32 (2011) 9374–9382

Contents lists available at SciVerse ScienceDirect

Biomaterials

journal homepage: www.elsevier.com/locate/biomaterials

The promotion of neurite sprouting and outgrowth of mouse hippocampal cells in culture by graphene substrates

Ning Li[a,c], Xuemin Zhang[a,d], Qin Song[a], Ruigong Su[a,c], Qi Zhang[a], Tao Kong[a], Liwei Liu[a,c], Gang Jin[b,c], Mingliang Tang[a,c,*], Guosheng Cheng[a,c,*]

[a] Suzhou Institute of Nano-Tech and Nano-Bionics, Chinese Academy of Sciences, 398 Ruoshui Road, Suzhou Industrial Park 215123, PR China
[b] Institute of Mechanics, Chinese Academy of Sciences, 15 Beisihuan West Road, Beijing, 100190, PR China
[c] Graduate University of the Chinese Academy of Sciences, 19A Yuquan Road, Beijing, 100049, PR China
[d] Changchun University of Science and Technology, Weixing Road, Changchun, Jilin, 130022, PR China

ARTICLE INFO

Article history:
Received 4 August 2011
Accepted 19 August 2011
Available online 8 September 2011

Keywords:
Neuron-favorable CVD graphene
GAP-43
Neurite sprouting & outgrowth
Hippocampus

ABSTRACT

Graphene has been demonstrated in many biomedical applications and its potentials for neural interfacing. Emerging concerns on graphene, as a biomedical material, are its biocompatibility and how biologically targeted tissue/cells respond to it. Relatively few studies attempted to address the interactions of graphene or its derivatives with the tissues/cells, while very few reports on neural system. In this study, we tried to explore how neurites, one of the key structures for neural functions, are affected by graphene during the development until maturation in a mouse hippocampal culture model. The results reveal that graphene substrates exhibited excellent biocompatibility, as cell viability and morphology were not affected. Meanwhile, neurite numbers and average neurite length on graphene were significantly enhanced during 2–7 days after cell seeding compared with tissue culture polystyrene (TCPS) substrates. Especially on Day 2 of the neural development period, graphene substrates efficiently promoted neurite sprouting and outgrowth to the maximal extent. Additionally, expression of growth-associate protein-43 (GAP-43) was examined in both graphene and TCPS groups. Western blot analysis showed that GAP-43 expression was greatly enhanced in graphene group compared to TCPS group, which might result in the boost of neurite sprouting and outgrowth. This study suggests the potential of graphene as a material for neural interfacing and provides insight into the future biomedical applications of graphene.

1. Introduction

Graphene, 2-dimensional monolayer of carbon atoms, has recently been considered as a promising candidate for the fabrication of ultrafast nanoelectronic devices, quantum computers, transparent electrodes, nanocomposite materials and biomedical materials due to its thermal, mechanical properties and electrical conductivity [1]. It has already been attempted to be used in a variety of biomedical applications, including cellular imaging and drug delivery [2], bio-analysis [3], stem cell research [4,5] and even photothermal therapy for tumor [6]. In terms of the biomedical applications of the graphene, nervous system would be an ideal breakthrough model. There are at least two reasons for this point. One is that neural cells are electro-active and functions of nerve system base on electrical activities. As neuronal stimulation and monitor are needed for a variety of clinical diagnostics and treatments [7–9], unique electrical properties of the graphene offer a great advantage for the therapeutic or other purposes. The other is that the electronic properties of the nanostructured graphene can be tailored to match the charge transport required for electrical cellular interfacing [10]. In addition, chemically stable properties of the graphene facilitate the integration with neural tissues. So far, considerable progress has already been made in this field, although solutions to many critical problems in neural biology/medicine are limited by the availability of specialized nanomaterials. For example, carbon nanotubes (CNTs) have been proved to be promising for neural electrode [11,12]. With those properties, graphene could also be expected to offer another opportunity to develop friendly and special-purpose interfacial materials for neural system, such as neural chips, implanted electrodes and drug/gene vectors.

* Corresponding authors. Suzhou Institute of Nano-Tech and Nano-Bionics, Chinese Academy of Sciences, 398 Ruoshui Road, Suzhou Industrial Park 215123, PR China.
E-mail addresses: mltang2010@sinano.ac.cn (M. Tang), gscheng2006@sinano.ac.cn (G. Cheng).

0142-9612/$ – see front matter © 2011 Elsevier Ltd. All rights reserved.
doi:10.1016/j.biomaterials.2011.08.065

Abbreviations

AFM	atomic force microscope
CNTs	carbon nanotubes
CVD	chemical vapor deposition
MTT	3-(4,5-Dimethyl-2-thiazolyl)-2,5-diphenyl-2H-tetrazolium bromide
GO	graphene oxide
GAP-43	growth-associate protein-43
LDH	lactase dehydrogenase
PLL	poly-L-lysine
rGO	reduced graphene oxide
TCPS	tissue culture polystyrene
XPS	X-ray photoelectron spectroscopy

Concerns about the graphene for the biomedical applications involve its biocompatibility and biological effects. Just like other nanomaterials used in biomedicine, this topic could be very tricky because of the differences of graphene synthesis techniques and the variety of the biological subjects studied. Despite of the challenges, for better understanding and better use of its biological effects, the graphene biocompatibility and interactions with an organism (tissue/cell) should be well clarified. Until now, there are a few studies on how different kinds of cells respond to graphene or its derivatives (graphene oxide (GO), reduced graphene oxide (rGO), graphene composite) and whether they are compatible with graphene or not. These subjects include cancerous cells, adherent mammalian cells, suspended cells and stem cells [2,5,13–20]. Though, complex interactions between graphene or its derivatives and these cells were observed, consensus on cellular toxicity about graphene or its derivatives is very much appreciated.

These previous work has inspired us to explore biological effects associated with graphene. Little is known about how graphene interacts with biological tissue/cells and how the biological target responds to graphene. In particular, there are few reports on the biological effects of graphene on nervous system or neurons, which is important for the development of graphene-based neural interfacing materials. Thus, in this study, we attempted to interpret the neuronal response to graphene substrates in a hippocampal culture model and determine the potential for applications within the nervous system.

2. Materials and methods

2.1. Materials

Copper foil was obtained from Alfa Aesar (Tianjing, China). Poly-L-lysine (PLL), Triton X-100, iron nitrate, 3-(4,5-Dimethyl-2-thiazolyl)-2,5-diphenyl-2H-tetrazolium bromide (MTT), monoclonal anti-β-tubulin antibody produced in mouse and monoclonal anti-GAP-43 antibody produced in rabbit were purchased from Sigma–Aldrich Corp. (St. Louis, USA). Cell culture reagents, goat anti-mouse IgG antibody labeled with Alexa Fluor®488 and goat anti-rabbit IgG antibody labeled Alexa Fluor®568 were supplied by Invitrogen Corp. (Shanghai, China), and CytoTox-ONE™ Homogeneous Membrane Integrity Assay kit was purchased from Promega (Beijing, China). ICR mice were acquired from SooChow University.

2.2. Substrate preparation

Graphene samples were synthesized according to previously published chemical vapor deposition (CVD) method [21]. Briefly, a thin copper foil (5 × 5 cm) was heated to 1000 °C and annealed for 20 min under H_2 and Ar gases, followed by exposure to H_2 and CH_4 for 5 min. Finally, the substrate was cooled down from 1000 °C to room temperature under H_2 and Ar gases. Graphene films were removed from the Cu foils by etching in an aqueous solution of iron nitrate. After the copper film was dissolved, a tissue culture polystyrene (TCPS) substrate was brought into contact with the graphene film and it was pulled from the solution, finally, a graphene/TCPS substrate was acquired using this method. TCPS substrate was cut from commercial TCPS dish for cell culture, and the graphene/TCPS substrates were

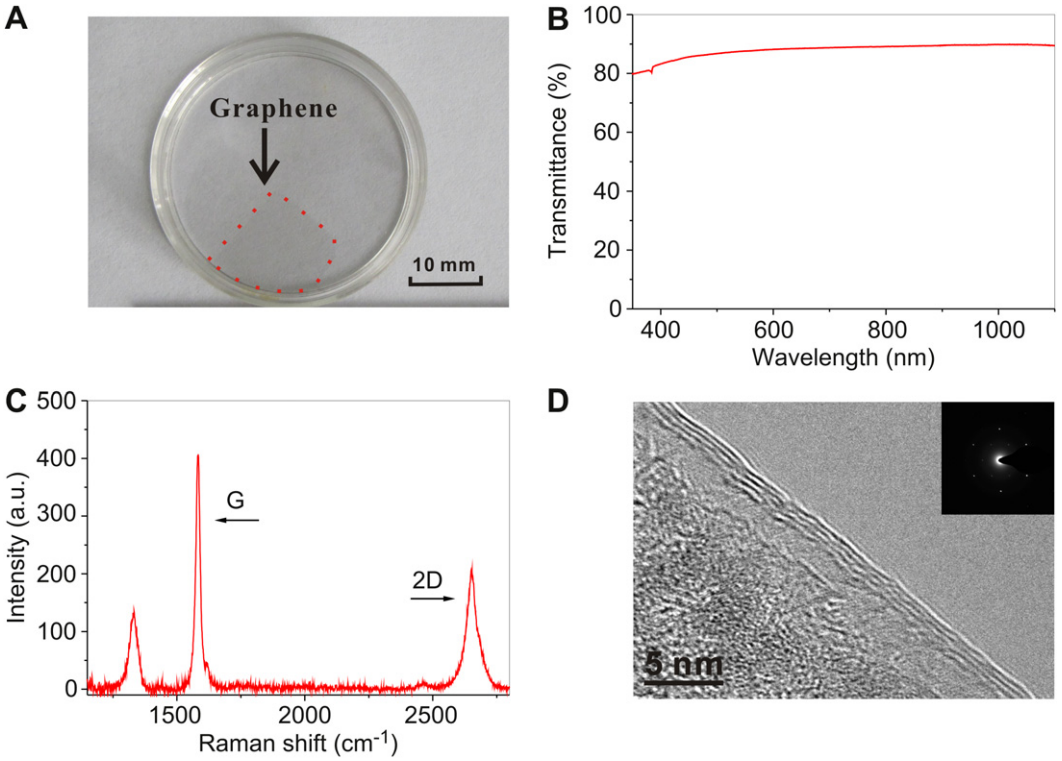

Fig. 1. Characterizations of CVD grown graphene film. (A) An optical image of the CVD grown graphene film transferred onto the bottom of TCPS dish, (B) Transmittance spectrum of CVD grown graphene film on glass microscope slide, (C) Micro-Raman spectrum of CVD grown graphene (incident laser wavelength: 632.8 nm, 100× objective), (D) Representative high-resolution TEM micrograph of the edge of graphene region consisting of four layers, selected-area electron diffraction pattern is inserted.

mounted with a chamber. Then, the device was immersed in milli-Q water overnight to remove residual soluble toxic components and in 75% ethanol solution for over 12 h for sterilization.

2.3. Surface modification of substrate

The substrates were coated with PLL (MW 150,000–300,000, 0.1 mg/mL) overnight in an incubator (37 °C, humid atmosphere with 5% CO_2), and thoroughly rinsed with sterile deionized water. Prior to cell culture, the substrates were incubated with complete culture medium overnight in an incubator.

2.4. Analysis of graphene substrates by UV/Vis spectroscopy, Raman spectroscopy, TEM, AFM, XPS and contact angle measurement

The graphene was transferred to TCPS dish for imaging. The transmittance of graphene was measured by UV/Vis spectrometer (lambda 25, PerkinElmer, Singapore). Glass microscope slides were cut into rectangles of 0.9 cm × 2.6 cm to fit into the sample holder. A blank glass slide was used as a reference for each measurement. The crystallinity and number of the layer presented within graphene were examined by Raman spectrometer (lamRAM HR800, HORIBA, France) and transmission electron microscope (TEM) (Tecnai G2 F20 S-Twin, FEI, USA). The surface morphologies of graphene and TCPS were determined by atomic force microscope (AFM) (Dimension 3100, Veeco, USA) using tapping mode operated at the room temperature. The surface chemistry of the substrates pre- and post-PLL modification was examined using X-ray photoelectron spectroscopy (XPS) (Axis Ultra DLD, Kratos, UK) utilizing an Al Ka X-ray source operated at 40 eV. The hydrophilicity of the substrates was evaluated, according to the sessile drop method, by measuring the water contact angles (CA) at different points for each sample.

2.5. Cell culture and characterization of neurons

The hippocampus of both hemispheres was dissected from the brain of postnatal day 1 ICR mouse, removed and collected in falcon tubes in 0.25% trypsin. The tissue was digested in trypsin for 15 min at 37 °C, and then gently triturated mechanically by using a sterile Pasteur pipette with a wide opening to dissociate larger aggregates. The cells were seeded at high density (25,000 cells/cm^2) for quantification of survival at 7 days *in vitro* and at low density (500 cells/cm^2) for measurement of neurite lengths *in vitro*. The cells were plated in DMEM-F12 medium containing 10% fetal calf serum, 2% B-27 supplement, penicillin–streptomycin, Ham's F-12 Nutrient Mixture. Cultures were maintained at 37 °C in humidified atmosphere with 5% CO_2 and half of the cell culture medium was replaced every 4 days.

The viability of neurons was observed by MTT assay and the membrane integrity of neurons was evaluated by using Lactase Dehydrogenase (LDH) assay, according to the protocol of CytoTox-ONE™ Homogeneous Membrane Integrity Assay kit. The assays were performed after 7-days culture, and data was recorded using a Multi-label Reader (Victor™×4, PerkinElmer, Singapore). The transparency characteristics of the substrates permitted an online observation of the cells with an inverse light microscope (Eclipse Ti-E, Nikon, Japan).

For imaging morphology of neurons on different substrates, cells were seeded on graphene and TCPS substrates. The morphology of neurons on the substrates was also examined with scanning electron microscopy (Inspect S, FEI, USA). For the sample preparation, neurons were prepared by fixation in 2.5% glutaraldehyde in pH 7.4 phosphate buffer, followed by post-fixation in 1% osmium tetroxide and by progressive dehydration in ethanol.

2.6. Neurite morphometry

From the second day (D2) to the seventh day (D7) after neurons were seeded, 6 well plate samples were analyzed via phase-contrast microscopy at 200× magnification. Micrographs of random areas of the culture plates were taken and subsequently analyzed with ImageJ (NIH, Bethesda, MD) for number of neurites per cell, length per neurite. For the growth characteristics, more than 150 cells were analyzed for each parameter for each experimental condition.

2.7. Immunofluorescence staining

The immunofluorescence experiments were conducted by using primary anti-β-tubulin and anti-GAP-43 antibodies and secondary antibody conjugated with Alexa

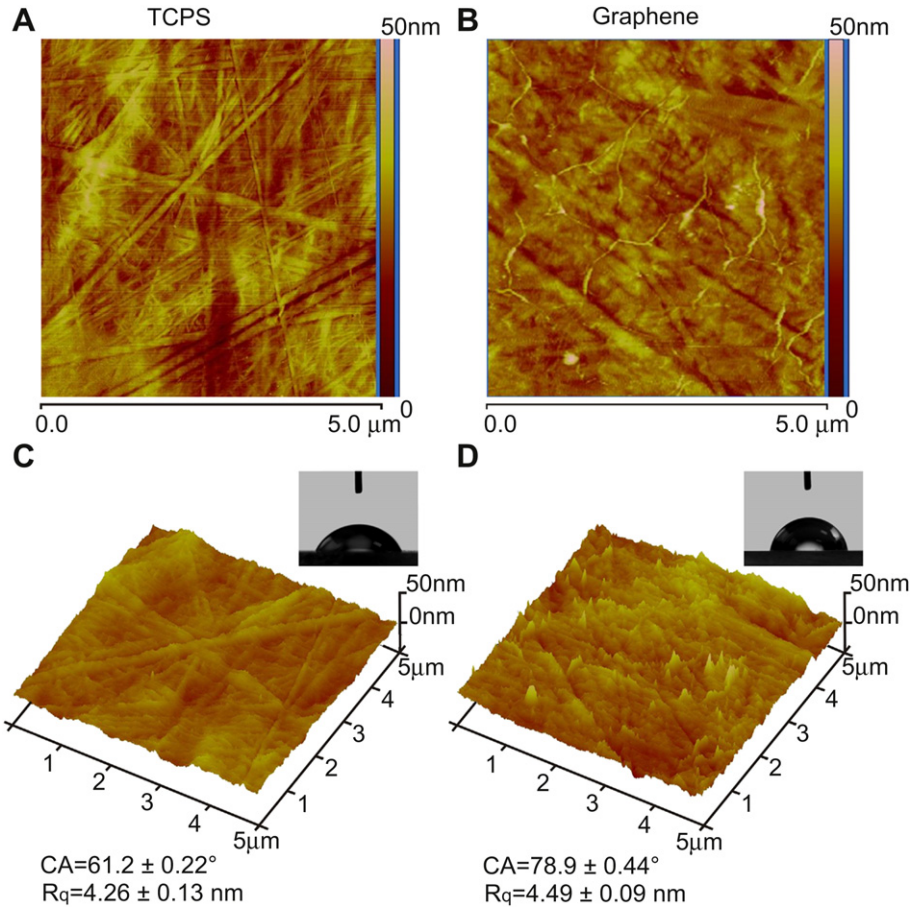

Fig. 2. Morphology and hydrophilicity of substrate surface. (A, C) AFM micrographs and contact angle measurement of TCPS. (B, D) AFM micrographs and contact angle measurement of graphene.

fluorochrome on samples previously fixed and permeabilized. Specifically, the neuronal cells were fixed in paraformaldehyde (4%) for 15 min. Fixed cells were permeabilized with 0.25% Triton X-100 in PBS for 10 min and subsequently blocked with 1% BSA for 30 min at room temperature. The cultures were then rinsed three times with PBS and incubated with the monoclonal antibodies anti-β-tubulin (1:200) and anti-GAP-43 (1:200) overnight at 4 °C. Afterwards, neuronal cells were rinsed with PBS and incubated with fluorescently labeled secondary antibodies Fluor®488-conjugated (1:200) and Fluor®568-conjugated (1:200) in PBS for 60 min at room temperature.

2.8. Western blot

Cells were harvested when they were mature on both graphene and TCPS substrates. A total of 50 μg of protein was loaded onto SDS-polyacrylamide gels and underwent electrophoresis at 160 V for 90 min. The separated protein was then transferred to a nitrocellulose membrane at 50 V for 1 h in a Tris-glycine transfer buffer (Invitrogen). The membrane were then blocked in 5% nonfat dry milk for 1 h and incubated overnight at 4 °C with anti-GAP-43 antibody (Sigma–Aldrich, 1:1000 dilution). Horseradish peroxidase conjugated goat anti-mouse IgG (ECL Kit; Amersham, Arlington Heights) was then applied for 1 h at room temperature. The blots were developed in luminal and exposed to Hyperfilm ECL (Amersham). The blots were stripped and normalized by re-probing with a gel loading (β-tubulin) control. The molecular weights were compared with prestained low-range standards (Bio-Rad).

2.9. Statistics

All data were presented as the mean ± standard error of the mean (SEM) of at least three independent experiments. Statistical analysis was performed using the two-way analysis of variance (ANOVA) test followed by a Tukey test (LST) to evaluate the statistical significance between the different groups. The significance levels were set at $^{*}p < 0.05$ and $^{**}p < 0.01$.

3. Results

3.1. Characterization of graphene

The graphene films produced in our experiments exhibited good characteristics of light transmission, which could be shown in an optical image of the graphene film transferred onto the bottom of TCPS dish (Fig. 1A). Fig. 1B shows that the graphene film had a nature of an optical transmittance (~90%) in 500–1000 nm wavelength regime. So, we speculated that the graphene film may contain about four layers, based on the relationship between the transmittance and the number of graphene layers [22]. This was further validated by room temperature micro-Raman spectroscopy, which is a nondestructive technique that could be used to characterize the crystallinity and the number of graphene layers. The full width at half-maximum (FWHM) of the 2D peak and the ratio between intensity of G and 2D bands (Fig. 1C) indicate that the graphene presented in this work contains about 3–5 layers [23–25].

The graphene film was transferred to TEM lacey carbon-coated grids for TEM imaging. The observation by TEM provides an accurate way to measure the number of layers at multiple locations on the film. Fig. 1D is a representative TEM micrograph of graphene film. Typically, sections of 3–5 layers were observed in our samples, which was consistent with our UV–Vis and Raman data. Selected-area electron diffraction of the graphene film (inset of Fig. 1D) revealed a hexagonal pattern of three-fold symmetry of the carbon

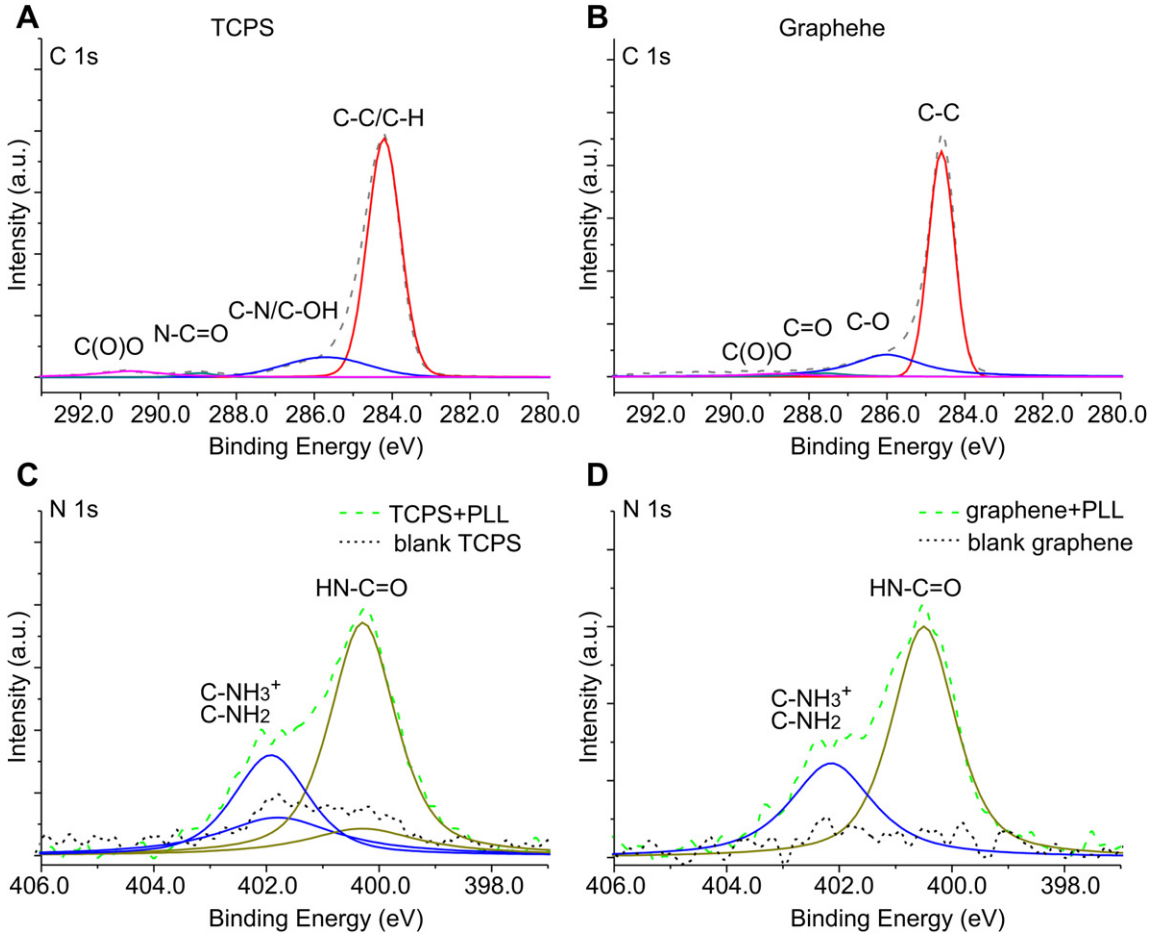

Fig. 3. High-resolution XPS spectra of blank TCPS and graphene. C (1s) peaks of blank TCPS (A) and graphene (B), N (1s) peaks of TCPS (C) and graphene (D) for pre- and post-PLL treatment.

atoms arrangement. When different regions of the film were inspected, well-defined diffraction spots (instead of ring patterns) were always observed, indicating the nature of high-quality crystallinity of all regions examined.

3.2. Surface characterization of substrate

Compared with TCPS, graphene substrate was consisted of many ripples and wrinkles on the micrometer scale imaged by AFM (Fig. 2), and such ripples and wrinkles are intrinsic to CVD grown graphene [26]. In order to quantify surface roughness, root mean square deviations (Rq) of two substrates by AFM were measured at 4.26 ± 0.13 nm and 4.49 ± 0.09 nm for the TCPS and graphene film, respectively, suggesting no significant differences in the surface roughness for these two substrates. According to the sessile drop method, the substrate hydrophilicity was evaluated. Fig. 2C and D inset shows the contact angles of TCPS and graphene film were $61.2 \pm 0.22^\circ$ and $78.9 \pm 0.44^\circ$, which implies that graphene is a little more hydrophobic than TCPS.

Furthermore, surface chemistry of the graphene films and TCPS was examined by XPS (Fig. 3). Carbon atoms are dominant element of TCPS and graphene. Various carbon-containing functional groups offer rational surface chemistry. In Fig. 3A and B, C1s XPS spectrum of TCPS shows four components that denote carbon atoms in four specific functional groups: non-oxygenated ring C, C in C–O bonds, carbonyl C, carboxylate carbon (O–C=O), respectively. In contrast, only two components were observed in the C1s XPS spectrum of the graphene. The main peak at 284.6 eV corresponds to the non-oxygenated ring C, while a small peak reflects C in C–O bonds. Compared with TCPS, graphene surface holds less oxygen-containing functional groups. PLL modification is believed to be useful for neuron growth. We can quantify PLL coverage by measuring N content (N1s XPS line) as N contained in the NH_3 groups forming the PLL molecule (Fig. 3C and D). The XPS study shows detectable content of nitrogen arising from PLL-modified graphene films compared to a native graphene films. The N1s atomic concentrations of the graphene surfaces for pre- and post-PLL modification are 0.68% and 2.78%, proving the success of PLL modification, which was further validated by presence of the N 1s peaks (HN–C=O, C–NH_2, C–NH_3^+) [27].

3.3. Neuron growth on graphene and TCPS substrates

From optical image of neurons (Fig. 4A), we observed that the presence of graphene did not influence neuron growth at all. The neurons cultured on graphene showed a similar morphology and density as on TCPS. The scanning electron microscopy image indicates that the neurons cultured on graphene had formed neurite networks after 7 days of culture, exhibiting normal adhesion and neurite formation (Fig. 4B). The result of MTT assays indicates that there was no significant difference in viability between neurons cultured on graphene and TCPS ($n = 9$, $p > 0.05$, Fig. 4C). Also, LDH assays could provide consistent result that graphene had no obvious impairment on the integrality of the cell membrane ($n = 9$, $p > 0.05$, Fig. 4D), as LDH release indicates membrane damage and is a hallmark of necrosis.

3.4. The number and length of neurites under developing period on graphene substrates

The neurons began to extend neurites into the periphery after being seeded on the substrates until they were mature. From D2 to D7 after neurons were seeded, the number of neurites and their length for most of neurons were calculated once a day. More than

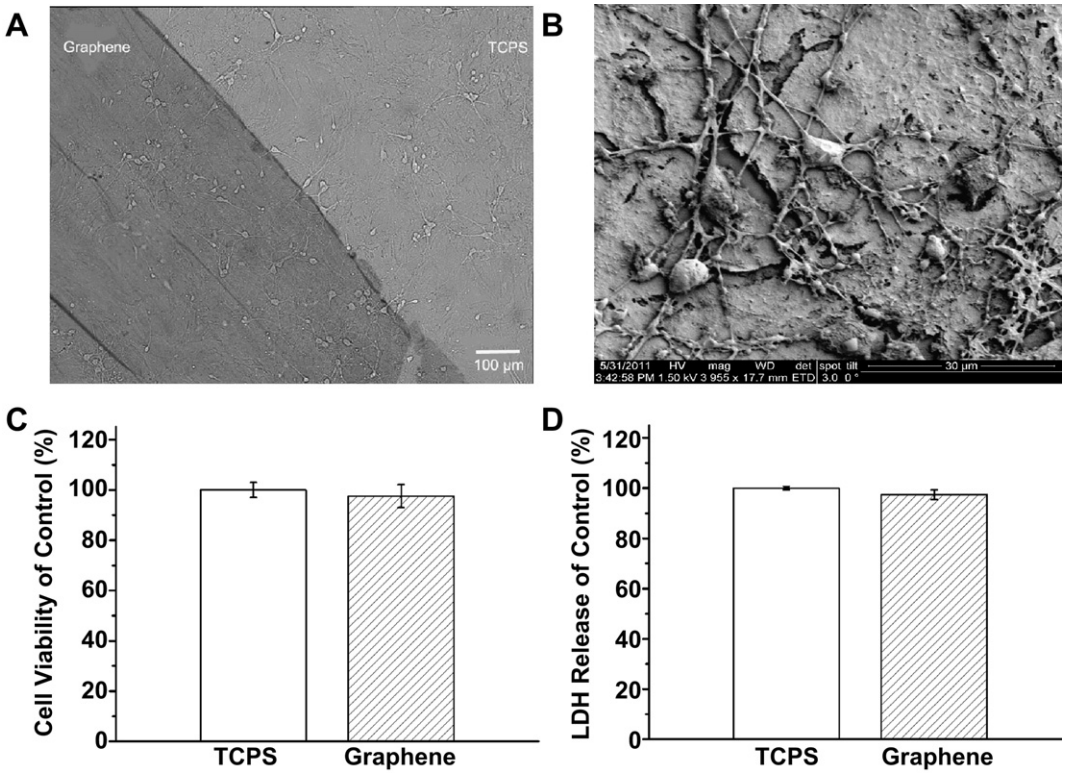

Fig. 4. Neurons cultured on different substrates. (A) An optical image of neurons cultured on the border of graphene (left) and TCPS (right), (B) scanning electron microscopy image of neurons on graphene, (C) MTT-measured viability of neurons cultured on TCPS and graphene after 7 days, (D) LDH activity of neurons after 7 days incubation on TCPS and graphene. Data are expressed as mean ± SEM ($n = 9$, $p > 0.05$).

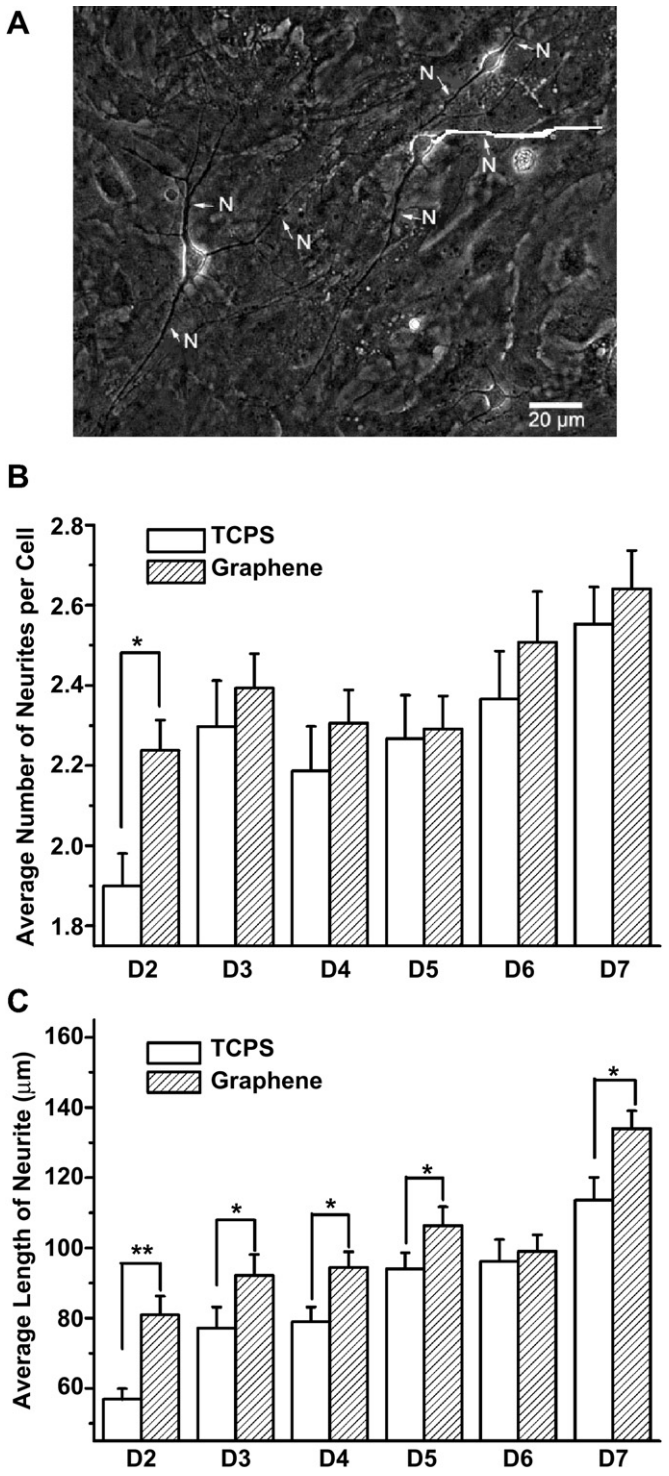

Fig. 5. Average numbers and length of neurites during developing period on TCPS and graphene. (A) Phase-contrast micrograph of typical neurons showing a trace along the extension of neurite (N) used for length calculation, (B) average number of neurites per neuron on TCPS and graphene during the developing period (D2–D7), (C) average neurite length of neuron on TCPS and graphene during the developing period (D2–D7). Data are expressed as mean ± SEM ($n = 315$ for graphene and $n = 288$ for TCPS, $^{**}p < 0.01$).

150 neurons were measured every day for each single group. As shown in Fig. 5B, the average numbers of neurites increased on graphene substrates compared to on TCPS from D2 to D7, but the significant difference could only be found on D2 ($n = 161$ for graphene and $n = 152$ for TCPS, $p < 0.05$). It indicates graphene substrates are capable of promoting neurite sprouting.

Meanwhile, the neurite lengths were also measured. The results show that the neurite lengths were gradually increased from D2 to D7 either on TCPS or on graphene (Fig. 5C) as expected, except for D6 on graphene (no significant difference between D5 and D6). During the developing period (D2–D7), the average length of neurites was longer on graphene than on TCPS, and most of them showed significant differences except for D6. Especially, the biggest difference took place on D2 ($n = 315$ for graphene and $n = 288$ for TCPS, $p < 0.01$). Then, frequency distribution of neurite lengths was statistically counted from D2 to D7 (Fig. 6). Briefly, neurite lengths were divided into six segments depending on their actual length, which included shorter than 25 μm, 25–50 μm, 50–75 μm, 75–100 μm, 100–150 μm and longer than 150 μm. It could be seen that shorter neurites appeared less and/or longer neurites appeared more on graphene substrates compared to on TCPS from D2 to D7 (Fig. 6A–F). Considering the results of the average neurite length and the frequency distribution, it is clear that neurites can grow faster on graphene than on TCPS.

3.5. GAP-43 expression in neurons

Growth-associated protein-43 is a neuronal protein associated with neurite outgrowth and has also been shown to be an efficient marker for the presence of neuronal growth cones [28]. To see whether boost of neurite outgrowth on graphene was related to GAP-43 upregulation or not, immunofluorescence and western blot experiments were carried out on D8 when neurons were mature. Fig. 7A demonstrates β-tubulin and GAP-43 immunofluorescence staining, which show brighter fluorescence for GAP-43 on graphene substrates compared to on TCPS. Further evidence came from the western blot experiment, as GAP-43 expression was significantly higher in graphene group than TCPS ($n = 3$/group, $p < 0.05$) (Fig. 7B and C). This suggests graphene substrates upregulate GAP-43 expression to promote neurite outgrowth.

4. Discussion

Biomedical applications of the graphene should start with its biocompatibility. Although discussion about the toxicity of graphene seems very difficult because of the differences in graphene itself and the experimental bio-subjects, there are still some works to quantify the cytotoxicity of graphene or its derivatives. Hu et al. reported that GO and rGO inhibited bacterial growth with minimal toxicity to human alveolar epithelial A549 cells [29]. Biris and coworkers demonstrated that graphene sheets induced dose-dependent cytotoxicity on phaeochromocytoma (PC12) cells [15]. On the contrary, other groups found high biocompatibility of GO or rGO. Ryoo et al. reported that GO and graphene substrates could improve gene transfection efficacy in NIH-3T3 fibroblasts without inducing cytotoxicity [13]. Also, graphene nanomaterials functionalized by macromolecules show good biocompatibility. In our study, no obvious cytotoxicity could be observed, as graphene did not significantly influence cell viability in a hippocampal culture model (Fig. 4C and D). The limited references above revealed no consensus on cellular toxicity of graphene or its derivatives. One likely source of this apparent disagreement is that the physicochemical properties of GO or graphene might not be always well controlled, which may induce different reactions on biological/toxicological activities. In our study, the CVD grown graphene was used, because great advances in CVD synthesis have allowed the preparation of sufficiently large area, high-quality graphene that are suitable for biological tests [21]. More importantly, CVD grown

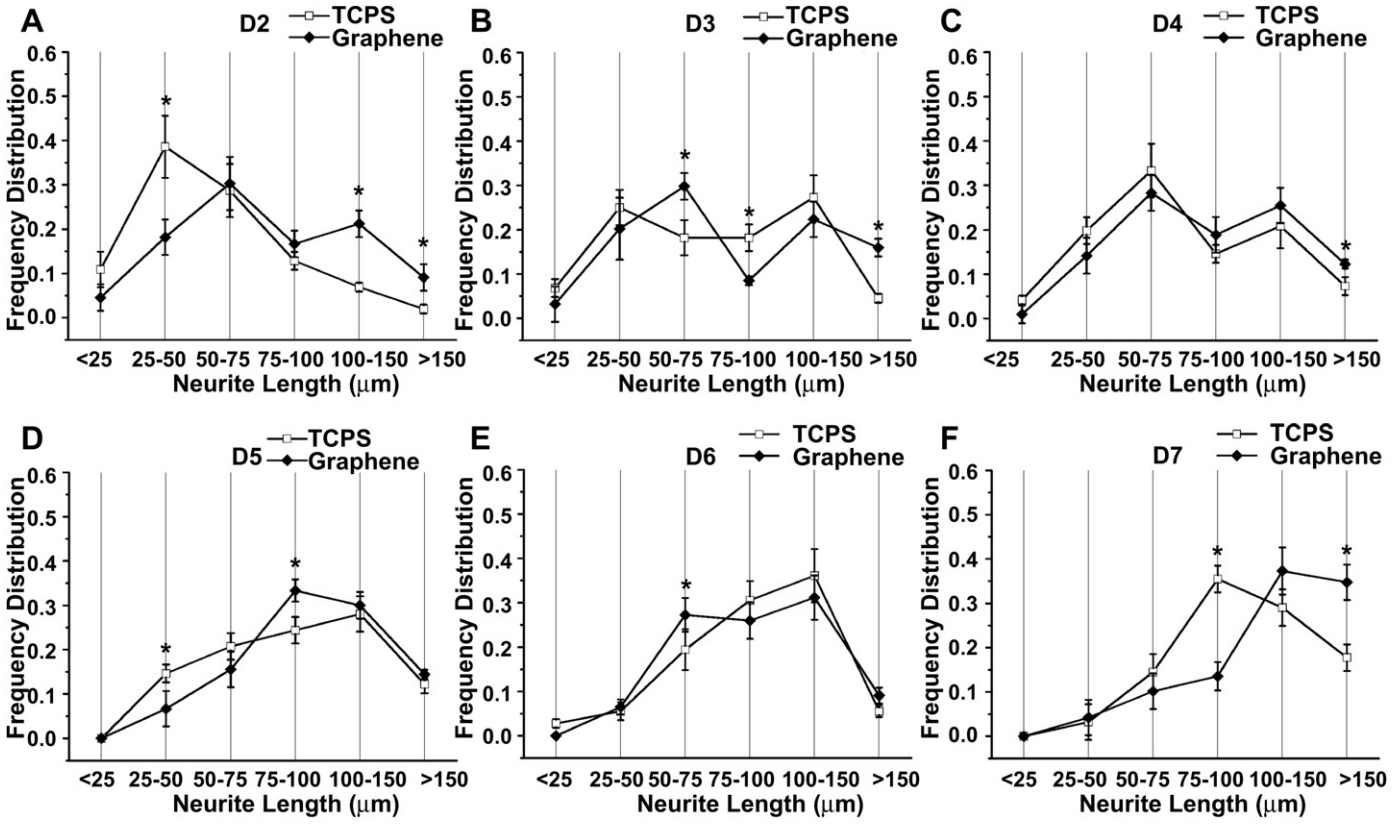

Fig. 6. Frequency distribution of neurite length of hippocampal neurons plated on TCPS and graphene during the developing period. (A) D2, (B) D3, (C) D4, (D) D5, (E) D6, (F) D7.

graphene remains intrinsic properties of graphene [30] and has simple topography and pure form.

Here, hippocampus was chosen to be the model of investigation, as it is an important brain area owing to its vital role in the consolidation of several forms of learning and memory and especially during the formation of declarative memories [31]. Hippocampal neurons, which are well known for their plasticity and regeneration properties, supply a best model for investigating the interactions between graphene and nervous system. In this work, graphene was shown to be neuron-favorable materials, as neurons could grow well, even better, on graphene substrates compared to on TCPS substrates (Fig. 4A). There may be several key issues for the friendly interaction of graphene with neurons. First of all, contamination by trace amounts of the catalyst often leads to formation of reactive oxygen species in CNTs [32], which may also happen to the graphene. In our experiment, catalyst Cu residual was examined by XPS, and the data shows that Cu content was undetectable after etching by an aqueous solution of iron nitrate and water immersion cleaning, while only trace amounts of Fe existed (Fe atomic concentration: 0.13%). Secondly, graphene substrates did not produce freely floating graphene sheet, while Barbaros Özyilmaz reported that graphene sheet remained intact during the cell culture process over 14 days [17]. Besides, the presence of small amounts of soluble toxic components should also be considered. At the beginning of the culture experiments, neurons did not grow well on the graphene substrates. By extending the time of water immersion cleaning, neuron state could be greatly improved. So, we speculate that soluble toxic components of graphene exist and can release to the cell culture medium during the culture, which may be effectively removed by a long-time water immersion cleaning. Moreover, PLL modification plays an important role in building the neuron-favorable substrates. From high-resolution XPS N (1s) spectrum of graphene film before and after PLL modification, we could found that the graphene film have been successfully coated with PLL (Fig. 3C and D). Due to its positive nature and high hydrophilicity, PLL coating is known to be a critical factor for success of cell culture, which may also contribute to good biocompatibility of graphene here. In addition to PLL modification, another important reason why neurons could grow well is that we soaked graphene substrate in medium containing serum overnight just before cell seeding. Huang reported that cytotoxicity of GO nanosheets arose from direct interactions between the cell membrane and GO nanosheets, which resulted in physical damage to the cell membrane. Also, they found that damage was largely attenuated when GO was incubated with fetal calf serum [20].

A neurite refers to any projection from the cell body of a neuron. This projection can be either an axon or a dendrite. The neurite sprouting and outgrowth is one of the symbols of development of nervous system [33]. It is rather remarkable that few-layer graphene was capable of promoting neurite sprouting and outgrowth of mouse hippocampal neurons, which could be verified by the data of average neurite numbers and length (Fig. 5). Especially, the statistical differences of average neurite number and length between graphene group and TCPS group were both biggest at D2 when compared with at D3–D7 (Figs. 5 and 6), which means graphene substrates may have a stronger impact on the early developing neurons. It is well known that neurons on the early developing stage are more sensitive to surrounding physical/chemical cues, which may result in more profound effects on D2. These results are almost certainly due to a complex interplay of mechanical, chemical and electrical cues imposed by graphene and it is hard to identify the microscopic origin of the effects of graphene on neurons.

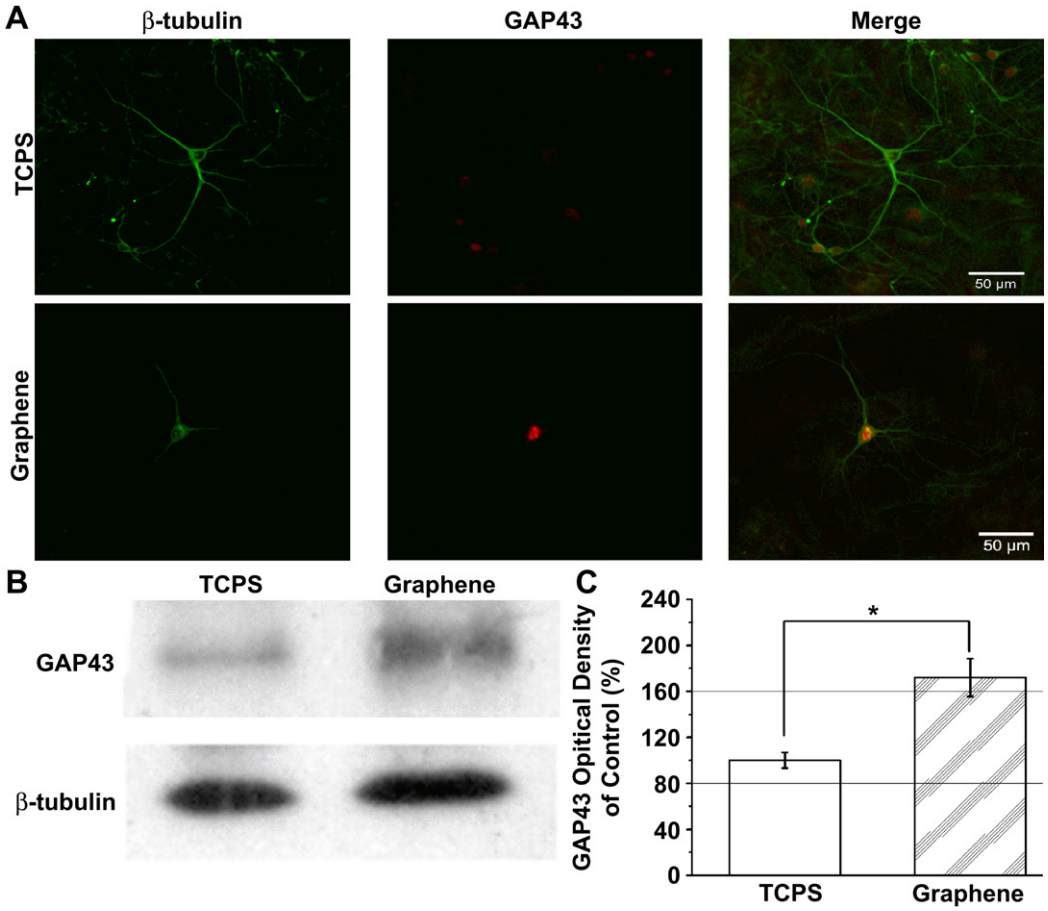

Fig. 7. (A) Confocal laser scanning micrographs of hippocampal neurons after 7 days of culture on TCPS and graphene. Neurons were stained for GAP-43 (red) and β-tubulin (green), (B) Western blot analysis of GAP-43 expression in neurons 7 days post neurons seeding on TCPS and graphene, (C) relative optical densities of GAP-43 bands shown in (B) ($n = 3$/group, $^{*}p < 0.05$) (for interpretation of the references to colour in this figure legend, the reader is referred to the web version of this article).

It was reported that substrate surface structure (surface roughness, topography, stiffness, etc.) has been shown to be very important in determining neuron–substrate interactions and influencing cell survival and neurite outgrowth. In this study, since the average roughness of graphene and TCPS surface have no obvious difference, as shown by AFM (Fig. 2), the effects of roughness may be neglected. It is worth noting that the topography of CVD grown graphene with its many ripples and wrinkles may mimic the surrounding matrix of neurons (Fig. 2B and D), which might provide positive substrates for neurons to grow. Meanwhile, surface chemistry plays a role in cellular interaction between neurons and substrates [34]. An increase of hydrophilicity is well correlated with an improved adhesion of neuronal cells onto the substrates [35]. However, we observed that the more hydrophobic graphene (Fig. 2D) promoted neurite growth, which may be due to the hydrophilicity change from complex interaction among graphene, PLL and chemicals in the culture medium. Additionally, surface chemical functional groups can influence the hippocampal neuron morphological development [36]. Finally, electrical phenomena play an important role in the nervous system, and it has been shown that the electrical conductivity of CNTs does promote neuron growth [37,38]. Based on these reports, it can be speculated that high electrical conductivity of graphene could also lead to better neurite outgrowth, but further evidence is still needed.

GAP-43 is a nervous tissue-specific cytoplasmic protein and is considered to participate in neurite formation and regeneration [39]. So, we tried to examine whether GAP-43 expression is affected by graphene or not. The results show that GAP-43 expression was significantly enhanced in graphene group compared in TCPS group (Fig. 7), which may explain why neurite sprouting and outgrowth of neurons could be promoted when seeded on graphene substrates. However, the underlying mechanisms of the enhancement of GAP-43 expression on graphene substrates need more delicate experiments to address.

5. Conclusions

We demonstrate here that CVD grown graphene films have excellent biocompatibility for primary culture of mouse hippocampal neurons and are even capable of promoting neurite sprouting and outgrowth, especially during the early developmental phase. Many neurodegenerative diseases or acute injuries to nervous system result in loss of neurons and damage of neurites, which calls for an easy and effective way to repair the damage of neurons. Due to these interactions of graphene with neurons, it may be potentially used as implanted materials or neural chips to provide a material for the tissue engineering, especially in the nervous system.

Acknowledgements

This work was partially funded by National Basic Research Program of China under award numbers of 2011CB965004, Fund for

Presidential Award Winners of Chinese Academy of Sciences (Y1BFS11001) and "100-Talents Program" of Chinese Academy of Sciences. This work was made possible by extraordinarily professional services by Nano-Fabrication & Nano-Characterization Platforms with Suzhou Institute of Nano-Tech and Nano-Bionics, Chinese Academy of Sciences. We thank Mr. Weiwei Li for the help of graphene synthesis.

References

[1] Zhu Y, Murali S, Cai W, Li X, Suk JW, Potts JR, et al. Graphene and graphene oxide: synthesis, properties, and applications. Adv Mater 2010;22:3906–24.
[2] Sun X, Liu Z, Welsher K, Robinson JT, Goodwin A, Zaric S, et al. Nano-graphene oxide for cellular imaging and drug delivery. Nano Res 2008;1:203–12.
[3] Cohen-Karni T, Qing Q, Li Q, Fang Y, Lieber CM. Graphene and nanowire transistors for cellular interfaces and electrical recording. Nano Lett 2010;10:1098–102.
[4] Kalbacova M, Broz A, Kong J, Kalbac M. Graphene substrates promote adherence of human osteoblasts and mesenchymal stromal cells. Carbon 2010;48:4323–9.
[5] Park SY, Park J, Sim SH, Sung MG, Kim KS, Hong BH, et al. Enhanced differentiation of human neural stem cells into neurons on graphene. Adv Mater; 2011. doi:10.1002/adma.201101503.
[6] Yang K, Zhang S, Zhang G, Sun X, Lee S-T, Liu Z. Graphene in mice: ultrahigh in vivo tumor uptake and efficient photothermal therapy. Nano Lett 2010;10:3318–23.
[7] Wilson BS, Lawson DT, Muller JM, Tyler RS, Kiefer J. Cochlear implants: some likely next steps. Annu Rev Biomed Eng 2003;5:207–49.
[8] Weiland JD, Liu WT, Humayun MS. Retinal prosthesis. Annu Rev Biomed Eng 2005;7:361–401.
[9] Navarro X, Krueger TB, Lago N, Micera S, Stieglitz T, Dario P. A critical review of interfaces with the peripheral nervous system for the control of neuroprostheses and hybrid bionic systems. J Peripher Nerv Syst 2005;10:229–58.
[10] Kotov NA, Winter JO, Clements IP, Jan E, Timko BP, Campidelli S, et al. Nanomaterials for neural interfaces. Adv Mater 2009;21:3970–4004.
[11] Keefer EW, Botterman BR, Romero MI, Rossi AF, Gross GW. Carbon nanotube coating improves neuronal recordings. Nat Nanotechnol 2008;3:434–9.
[12] Mazzatenta A, Giugliano M, Campidelli S, Gambazzi L, Businaro L, Markram H, et al. Interfacing neurons with carbon nanotubes: electrical signal transfer and synaptic stimulation in cultured brain circuits. J Neurosci 2007;27:6931–6.
[13] Ryoo S-R, Kim Y-K, Kim M-H, Min D- H. Behaviors of NIH-3T3 fibroblasts on graphene/carbon nanotubes: proliferation, focal adhesion, and gene transfection studies. ACS Nano 2010;4:6587–98.
[14] Park S, Mohanty N, Suk JW, Nagaraja A, An JH, Piner RD, et al. Biocompatible, robust free-standing paper composed of a TWEEN/graphene composite. Adv Mater 2010;22:1736–40.
[15] Zhang Y, Ali SF, Dervishi E, Xu Y, Li Z, Casciano D, et al. Cytotoxicity effects of graphene and single-wall carbon nanotubes in neural phaeochromocytoma-derived PC12 cells. ACS Nano 2010;4:3181–6.
[16] Zhang L, Xia J, Zhao Q, Liu L, Zhang Z. Functional graphene oxide as a nanocarrier for controlled loading and targeted delivery of mixed anticancer drugs. Small 2010;6:537–44.
[17] Nayak TR, Andersen H, Makam VS, Khaw C, Bae S, Xu X, et al. Graphene for controlled and accelerated osteogenic differentiation of human mesenchymal stem cells. ACS Nano 2011;5:4670–8.
[18] Chang Y, Yang ST, Liu JH, Dong E, Wang Y, Cao A, et al. In vitro toxicity evaluation of graphene oxide on A549 cells. Toxicol Lett 2011;200:201–10.
[19] Chen H, Müller MB, Gilmore KJ, Wallace GG, Li D. Mechanically strong, electrically conductive, and biocompatible graphene paper. Adv Mater 2008;20:3557–61.
[20] Hu W, Peng C, Lv M, Li X, Zhang Y, Chen N, et al. Protein corona-mediated mitigation of cytotoxicity of graphene oxide. ACS Nano 2011;5:3693–700.
[21] Li X, Cai W, An J, Kim S, Nah J, Yang D, et al. Large-area synthesis of high-quality and uniform graphene films on copper foils. Science 2009;324:1312–4.
[22] Nair RR, Blake P, Grigorenko AN, Novoselov KS, Booth TJ, Stauber T, et al. Fine structure constant defines visual transparency of graphene. Science 2008;320:1308.
[23] Dervishi E, Li Z, Watanabe F, Biswas A, Xu Y, Biris AR, et al. Large-scale graphene production by RF-cCVD method. Chem Commun; 2009:4061–3.
[24] Ferrari AC, Meyer JC, Scardaci V, Casiraghi C, Lazzeri M, Mauri F, et al. Raman spectrum of graphene and graphene layers. Phys Rev Lett 2006;97:187401.
[25] Graf D, Molitor F, Ensslin K, Stampfer C, Jungen A, Hierold C, et al. Spatially resolved raman spectroscopy of single- and few-layer graphene. Nano Lett 2007;7:238–42.
[26] Sudibya HG, Ma J, Dong X, Ng S, Li L-J, Liu X-W, et al. Interfacing glycosylated carbon-nanotube-network devices with living cells to detect dynamic secretion of biomolecules. Angew Chem Int Edit 2009;48:2723–6.
[27] Tam SK, Dusseault J, Polizu S, Ménard M, Hallé J-P, Yahia LH. Physicochemical model of alginate-poly-l-lysine microcapsules defined at the micrometric/nanometric scale using ATR-FTIR, XPS, and ToF-SIMS. Biomaterials 2005;26:6950–61.
[28] Meiri KF, Pfenninger KH, Willard MB. Growth-associated protein, GAP-43, a polypeptide that is induced when neurons extend axons, is a component of growth cones and corresponds to pp46, a major polypeptide of a subcellular fraction enriched in growth cones. Proc Natl Acad Sci USA 1986;83:3537–41.
[29] Hu W, Peng C, Luo W, Lv M, Li X, Li D, et al. Graphene-based antibacterial paper. ACS Nano 2010;4:4317–23.
[30] Reina A, Jia X, Ho J, Nezich D, Son H, Bulovic V, et al. Large area, few-layer graphene films on arbitrary substrates by chemical vapor deposition. Nano Lett 2008;9:30–5.
[31] Lynch MA. Long-term potentiation and memory. Physiol Rev 2004;84:87–136.
[32] Firme Iii CP, Bandaru PR. Toxicity issues in the application of carbon nanotubes to biological systems. Nanomed-Nanotechnol Biol Med 2010;6:245–56.
[33] Rogers SL, Letourneau PC, Palm SL, McCarthy J, Furcht LT. Neurite extension by peripheral and central nervous system neurons in response to substratum-bound fibronectin and laminin. Dev Biol 1983;98:212–20.
[34] Cyster LA, Grant DM, Parker KG, Parker TL. The effect of surface chemistry and structure of titanium nitride (TiN) films on primary hippocampal cells. Biomol Eng 2002;19:171–5.
[35] Massia SP, Holecko MM, Ehteshami GR. In vitro assessment of bioactive coatings for neural implant applications. J Biomed Mater Res Part A 2004;68:177–86.
[36] Stenger DA, Pike CJ, Hickman JJ, Cotman CW. Surface determinants of neuronal survival and growth on self-assembled monolayers in culture. Brain Res 1993;630:136–47.
[37] Hu H, Ni Y, Montana V, Haddon RC, Parpura V. Chemically functionalized carbon nanotubes as substrates for neuronal growth. Nano Lett 2004;4:507–11.
[38] Malarkey EB, Fisher KA, Bekyarova E, Liu W, Haddon RC, Parpura V. Conductive single-walled carbon nanotube substrates modulate neuronal growth. Nano Lett 2009;9:264–8.
[39] Benowitz LI, Routtenberg A. GAP-43: an intrinsic determinant of neuronal development and plasticity. Trends Neurosci 1997;20:84–91.